Life Sciences 370 (2025) 123524

Contents lists available at ScienceDirect

Life Sciences

journal homepage: www.elsevier.com/locate/lifescie

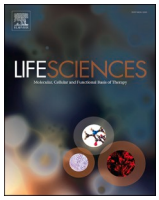

The interplay between COVID-19 and heart disease: Unravelling a complex connection

G.D. Duerr [a,*,1], M. Hamiko [b,1], J. Beer [a,1], J. Nattermann [c], M. Schafhaus [b], S.A.E. Held [d], J.C. Schewe [e], M. Wittmann [f], C. Kurts [g], S. Zimmer [h], M. Velten [i,1], A. Heine [d,1]

[a] Department of Cardiovascular Surgery, University Medical Center, Johannes-Gutenberg University, Mainz, Germany
[b] Department of Cardiac Surgery, University Hospital Bonn, Bonn, Germany
[c] Department of Internal Medicine I, University Hospital Bonn, Bonn, Germany
[d] Department of Internal Medicine III for Hematology, Oncology, Rheumatology and Immune-Oncology, University Hospital Bonn, Bonn, Germany
[e] Department of Anesthesiology, Intensive Care Medicine and Pain Therapy, University Medical Center Rostock, Rostock, Germany
[f] Department of Anesthesiology and Intensive Care Medicine, University Hospital Bonn, Bonn, Germany
[g] Institute for Experimental Immunology, University Hospital Bonn, University of Bonn, Bonn, Germany
[h] Department of Internal Medicine II – Cardiology, University Hospital Bonn, Bonn, Germany
[i] Department of Anesthesiology and Pain Management, The University of Texas Southwestern Medical Center, Dallas, TX, USA

ARTICLE INFO

Keywords:
COVID-19
SARS-CoV-2
Heart disease
Prognostic factors
Artificial intelligence

ABSTRACT

The intersection of coronavirus (COVID-19) and heart disease has emerged as a critical nexus in the landscape of global health. Individuals with heart disease face elevated risks when infected with Severe Acute Respiratory-Syndrome Coronavirus-type-2 (SARS-CoV-2) leading to COVID-19. The virus can directly affect the heart, resulting in myocarditis, arrhythmias, and heart failure, even in individuals without prior medical cardiac history. Therefore, tools identifying patients with cardiac infestation and predicting disease severity are of utmost importance. This study's unbiased stratification of clinical and immunological parameters of 134 SARS-CoV-2 positive patients revealed clusters of course-severity within the established WHO ordinal severity-scale leading to its summary (SWOSS) into three categories, A-C. PE and SWOSS-C were significantly associated with reduced survival of COVID-19 patients. The previously introduced CD8/Treg/monocyte-ratio which hints at a dysfunctional antiviral immunity associated with poor prognosis could be verified in this larger study population. However, the number of circulating CD14 + HLA-DR+ monocytes represented the most significant predictor for myocardial damage indicated by PE. We used all available data for an unbiased examination of associations and predictions by machine learning algorithms: Predictive markers for PE can be obtained in clinic and may serve as prognostic features. Among numerous parameters, C-reactive protein (CRP) was the most important in determining the presence of PE and SWOSS-category. Prediction of survival was most relevantly influenced by SWOSS-category underlining the benefit of this condensed classification for clinical practice. All AI-revealed prognostic features serve as promising starting-point to gain further understanding of the interplay between COVID-19 and heart disease.

1. Introduction

Coronavirus disease 2019 (COVID-19) associated cardiac injury has been abundantly observed in clinical practice and was repeatedly described as a predictor for poor outcome due to a more severe course of disease. [1,2] While patients with preexisting heart conditions presented with additional myocardial damage upon clinical apparent Severe Acute Respiratory Syndrome Coronavirus type 2 (SARS-CoV-2) infection, cardiac infestation could be observed in individuals in the absence of preexisting heart disease, also. [3,4] COVID-19 related myocardial injury may result in arrhythmia, heart failure, or sudden cardiac arrest. [4–6]

* Corresponding author at: Department of Cardiovascular Surgery, University Medical Center of the Johannes Gutenberg University of Mainz, Langenbeckstraße 1, 55131 Mainz, Germany.
E-mail address: danduerr@uni-mainz.de (G.D. Duerr).
[1] These authors contributed equally to this work.

https://doi.org/10.1016/j.lfs.2025.123524
Received 10 December 2024; Received in revised form 23 February 2025; Accepted 1 March 2025
Available online 3 March 2025

While the underlying pathomechanisms of COVID-19 related cardiac damage have not yet been revealed in total, direct SARS-CoV-2-infestation of cardiomyocytes as well as systemic reactions (e.g., cytokine storms, endothelial dysfunction) to COVID-19 have been proven to play a role in cardiac impairment. [7–10] Even though, investigation of SARS-CoV-2 induced acute myocarditis (AM) and pericarditis (AP) is impeded by significant numbers of pauci- and asymptomatic cases, in a large retrospective cohort study ($n = 211{,}619$) Li et al. determined the incidence of AP in COVID-19 patients to 0.46 %. [11,12]

Despite this overall low rate of occurrence, increased mortality, greater risks of renal failure, congestive heart failure, cardiogenic shock, and cardiac arrest as well as higher health care costs could be observed in AP patients, confirming the findings of previous, pioneering studies and case reports. [1,13,14] Therefore, prediction of cardiac damage in COVID-19 patients appears to be obligatory for effective medical care and risk stratification. However, robust parameters and risk factors predicting myocardial involvement during SARS-CoV-2 infection are still sought-for.

This study aims to identify key features, derived from clinical data, high-throughput screenings, and disease progression, that most effectively predict patient risk and potential outcomes. We found sets of factors with high potential in serving in clinical diagnostics.

2. Material and methods

2.1. Data collection

After approval from the Ethics Committee at the University Hospital Bonn, Germany (No.: 107/20) and in accordance with the Declaration of Helsinki and §15 of the Medical Association Nordrheins' professional code of conduct, 134 patients were enrolled upon administration to University Medical Center Bonn with symptoms typical for SARS-CoV-2 infection. Infection was confirmed by smear test for SARS-CoV-2 RNA according to WHO standards. Next to routine clinical and laboratory diagnostics, the immunological phenotype of every patient was characterized by Taqman® RT-qPCR (qPCR)-, Luminex- and FACS-analyses according to standard protocols as previously described. [1] All patients were followed up until hospital discharge or death. Data were recorded by our patient data management system and statistically analyzed as described in detail in the following.

2.2. Group definition

To streamline clinical relevance, the established WHO ordinal severity scale was subsumed into group A (no ventilation/no high-flow oxygen = WHO 1–4), B (non- or invasive ventilation = WHO 5–6), and C (organ support [e.g. catecholamines, extracorporeal life support (ECLS)/extracorporeal membrane oxygenation (ECMO)] or death = WHO 7–8). In the following, it is referred to as SWOSS (summarized WHO ordinal severity scale).

2.3. Data cleanup

To ensure high quality and reliability of results, we performed a comprehensive data cleanup procedure to prepare the dataset for further analysis. The data cleanup process involved several steps:

First, we removed features with redundant information. Any features that contained identical or redundant information were identified and only a single feature was kept as representative of the other redundant features. This step ensured that only unique and relevant information was retained for subsequent analysis.

High collinearity among features can lead to multicollinearity issues in statistical models. To address this, we performed a correlation analysis and identified features with a Spearman correlation coefficient higher than 0.85. In such cases, only one feature was retained, while the others were removed from the dataset. This step reduced redundancy and improved the interpretability of the data.

Missing data can significantly impact the quality of the analysis. Features with more than 25 % of the patient records containing missing values were considered unreliable and therefore removed from the dataset.

In consultation with clinicians, the dataset was thoroughly reviewed for any unusual patterns or anomalies, such as copied values across patients. Any such discrepancies were identified and corrected, ensuring the accuracy of the data.

Data may occasionally be mis formatted, which can lead to erroneous results. Mis formatted data points were identified and corrected to ensure that the dataset was free from data entry errors or inconsistencies.

Outliers can significantly affect the accuracy and robustness of statistical analyses. In this study, we employed an outlier detection procedure to identify extreme outliers within the dataset. The following steps were followed:

Z-Scaling: To make the dataset's features comparable, all continuous features were z-scaled, ensuring a mean of 0 and a standard deviation of 1.

Extreme Outlier Identification: Extreme outliers were identified based on z-scaled values. Any data point with a z-scaled value greater than 4, where this value was ranked as the largest value for the respective feature, was considered an extreme outlier. These data points were marked as 'NA,' indicating that they required special attention and possible imputation in subsequent analyses.

A statistical summary of the data used in this study can be found in Supplementary Table 2.

This cleaned dataset was used for all plots generated in Figs. 2 and 3. Prior to imputation of missing data, the features of the Luminex data were processed using the transformation function 'asinh' available in the R base functions. Before applying the imputation, we rigorously removed dependent features to avoid collinearity while computing missing data. We applied the 'mice'R package to model the missing data. We applied 5 iteration rounds and used the default imputation methods. After the imputation was done, we used the 'loess' normalization for the Luminex data by utilizing the 'LumiN' function of the 'lumi' R package.

A statistical summary of the imputed data can be found in Supplementary Table 3.

2.4. Kaplan-Meier curves

The cleaned data was used as input to Kaplan-Meier curves. The goal of this analysis was to assess survival status in relation to two key features, 'pericardial effusion' and 'WHO categories'. The analysis was performed using the 'survfit' function from the R package 'survival'.

2.5. Chi-square testing

After cleaning the data and extracting categorical features, the Chi-square test of independence was conducted using R's chisq. test function. To investigate associations between categorical factors and outcomes such as survival, WHO SWOSS category, or the presence of PE, each categorical feature was binarized into "present" [1] or "not present" (0). For each binarized variable, we constructed a 2×2 contingency table (or a 2×3 contingency table in cases where WHO SWOSS categories were the outcome) to compare the distribution of feature presence or absence with the respective outcome. Pearson residuals were calculated from these tables using again the chisq. test function. For visualization, Pearson residuals for the "presence" events were plotted.

2.6. Dimensionality reduction and consensus clustering

The continuous features of the imputed data were used as input to dimensionality reduction. First, the variance of the data was stabilized

by applying z-score on the values. The 'PCA' function of the R package 'FactoMineR' was applied on the transformed dataset. The first 20 computed PCs were used as input into the 'umap' function of the 'uwot' R package, by setting the 'n_neighbors' argument to 8. Next, we investigated the formation of stable clusters in the dimensionality reduced dataset. To not rely on a single method, we applied consensus clustering to identify the most stable patient clusters. To this end, we used the 'dice' function of the 'diceR' package. We set the number of requested clusters to the range 3–10. As cluster algorithms we used 'hdbscan', 'pam', 'gmm', and 'cmeans'. Finally, we set the 'cons.funs' argument to 'kmodes', 'majority', 'CSPA', and 'LCE'. Finally, we extracted the features that were most closely associated with the identified clusters. To ensure that the identified clusters were not artefacts of dimensionality reduction, we applied the consensus clustering strategy to the complete scaled dataset without performing any prior dimensionality reduction. The number of clusters was set to four, consistent with the cluster number identified through consensus clustering of the UMAP-reduced data. We then used a Sankey plot to assess whether samples in the UMAP-based clustering were consistently grouped in the clustering derived from the full dataset. The Sankey plot demonstrated that the majority of patients were assigned to the same clusters, irrespective of whether clustering was performed on the UMAP-reduced data or the complete dataset (Supplementary Fig. 1). Thus, we applied Wilcoxon test between a respective cluster versus all other identified clusters.

2.7. Random forest modelling

For the random forest modelling, we used non-scaled data. We modeled Random Forest trees on non-longitudinal data. Thus, reoccurring patients in the dataset were excluded. As dependent variables, we define 'pericardial effusion' and 'WHO category'. We split the data by using 60 % of the patients as training dataset and the remaining 40 % as validation dataset. We trained the random forest trees by using the 'randomForest' function of the R package 'randomForest'. We set the function argument 'ntree' to 500 and confirmed that the feature importance was assessed. In addition, we identified the optimal value for the parameter ('mtry') to define the number of variables randomly sampled as candidates at each tree split, by iterating through a value range and assessing the resulting error rate of the modeled random forests. To identify the most important features identified by the random forest trees, we extracted the feature importance represented by mean decrease accuracy. We set a cutoff of 0.002 to define a feature of being important for the prediction of the respective dependent variables. For validation, we applied logistic regression based on the identified features using the 'glm' function of the R package collection 'stats'. We visualized the quality of the models using ROC curves and calculated the area under der curve (AUC).

2.8. Statistical analysis and data visualization

In general, 'pheatmap' and the 'ggplot2' package were used to generate figures. If not otherwise stated, for continuous two-condition comparison Wilcoxon rank-sum test was used and for multi-condition comparison a Kruskal-Wallis test was performed. For categorical comparisons, a Chi-square test was applied.

3. Results

The dataset of this study consists of continuous data (mainly data that were obtained by experimental and routine lab experiments) and discrete data (comorbidities, usage of therapies or presence of clinical endpoints). Unbiased stratification predicting clinical outcome was performed according to the strategy illustrated in Fig. 1B. First, upon collection of patients´clinical and laboratory data (Fig. 1A), we used the continuous data to check, whether we could identify clusters in a high-dimensional space. Data-driven clustering resulted in 4 groups, of which cluster 1 and 4 resembled patients with moderate, while cluster 3 represented individuals with mild and 2 with poor clinical outcome (Fig. 1C,D). Interestingly, the stratified patients met the criteria of the SWOSS (Fig. 1D top, Supplementary Fig. 1) and clusters were in line with the SWOSS's prediction of survival (Fig. 1D bottom). The following analyses were carried out resting upon the summarized classification (SWOSS categories), accordingly. Features being differential for unbiased clustering were depicted with reference to their relevance (Fig. 1E). Of note, immature granulocytes were, next to common laboratory markers of inflammation (CRP, IL-6), significantly associated with Cluster 2 and therefore SWOSS C (Fig. 1E) confirming the previously reported relevance of immature granulocytes as a prognostic parameter for COVID-19 severity. [15,16]

3.1. Association of SWOSS and PE with survival after SARS-CoV-2-infection

Next, we investigated how the SWOSS category is associated with the discrete parameters (Fig.2). In addition, we also used the presence of PE as an endpoint, as it was found to be commonly associated with severe COVID-19 and survival status. [1] Pearson residuals were determined and depicted as dot plots (Fig. 2). A strong association could be observed between SWOSS-category and the presence of PE (Chi-square p = 2.453e-12). Next to the SWOSS-defining features ECMO support therapy and ventilation, renal failure was mildly (Chi-square $p = 0.0575$), while respiratory failure (RF) was strongly associated with SWOSS C (Chi-square $p = 1.321e-15$) and PE (Chi-square $p = 9.812e-08$). Interestingly, previous cardiac surgery and prevalence of heart valve disease were positively associated with PE (Chi-square $p = 0.01215$) and SWOSS C (Chi-square $p = 0.0001563$), while minimal association with survival (Chi-square p = 1) could be observed for these features.

Mortality was strongest associated with ECMO support therapy (Chi-squared $p = 5.423e-06$), ventilation (Chi-squared $p = 2.603e-06$), and RF (Chi-squared $p = 5.625e-06$), underlining these features´relevance as stand-alone risk factors.

3.2. Outcome and confirmation of previously published indicators for disease severity

In our previous study published in 2020, presence of PE could be detected as a parameter predicting a more severe course of COVID-19. [1] Results from the present, larger, and more thoroughly investigated study cohort are depicted in the Kaplan Meier plot (Fig. 3A), confirming that survival probability of COVID-19 patients with PE was significantly reduced (log-rank test $p = 0.0001$). Furthermore, a higher SWOSS-category was also associated with higher mortality (log-rank test p = 0.0001; Fig. 3B). Therefore, both features were considered as effective prognostic parameters in the context of COVID-19 for clinical practice. Interestingly, PE dimensions were significantly greater in patients with higher SWOSS (Fig. 3C).

APACHE II-score and CCL 2-concentration were significantly higher in PE patients (Fig. 3D, E), while IFN-γ levels were significantly lower in PE patients (Wilcoxon $p = 0.0033$; Fig. 3F). Whereas no significant difference in maximum troponin T (all time high) could be observed between PE and no PE individuals (Fig. 3G), patients in WHO category B and C showed significantly greater levels of serum troponin T (maximum all time high) compared to group A (Fig. 3H). Except for serum troponin T in PE and no PE patients, all results were in line with the observed outcome of the study from 2020; Moreover, in 2020 the CD8/Treg/monocyte ratio could be unraveled as an immunological marker for poor prognosis of COVID-19 patients. [1] While in this study the elevation of the CD8/Treg/monocyte ratio in PE patients could be confirmed (Fig. 3I), the number of CD14 + HLA-DR+ monocytes alone was even more significantly reduced in PE patients (Wilcoxon p = 1,2e-07; Fig. 3I```). Therefore, we concluded that the combination of monocytes with CD8+ T cells and regulatory T cells did not achieve a better

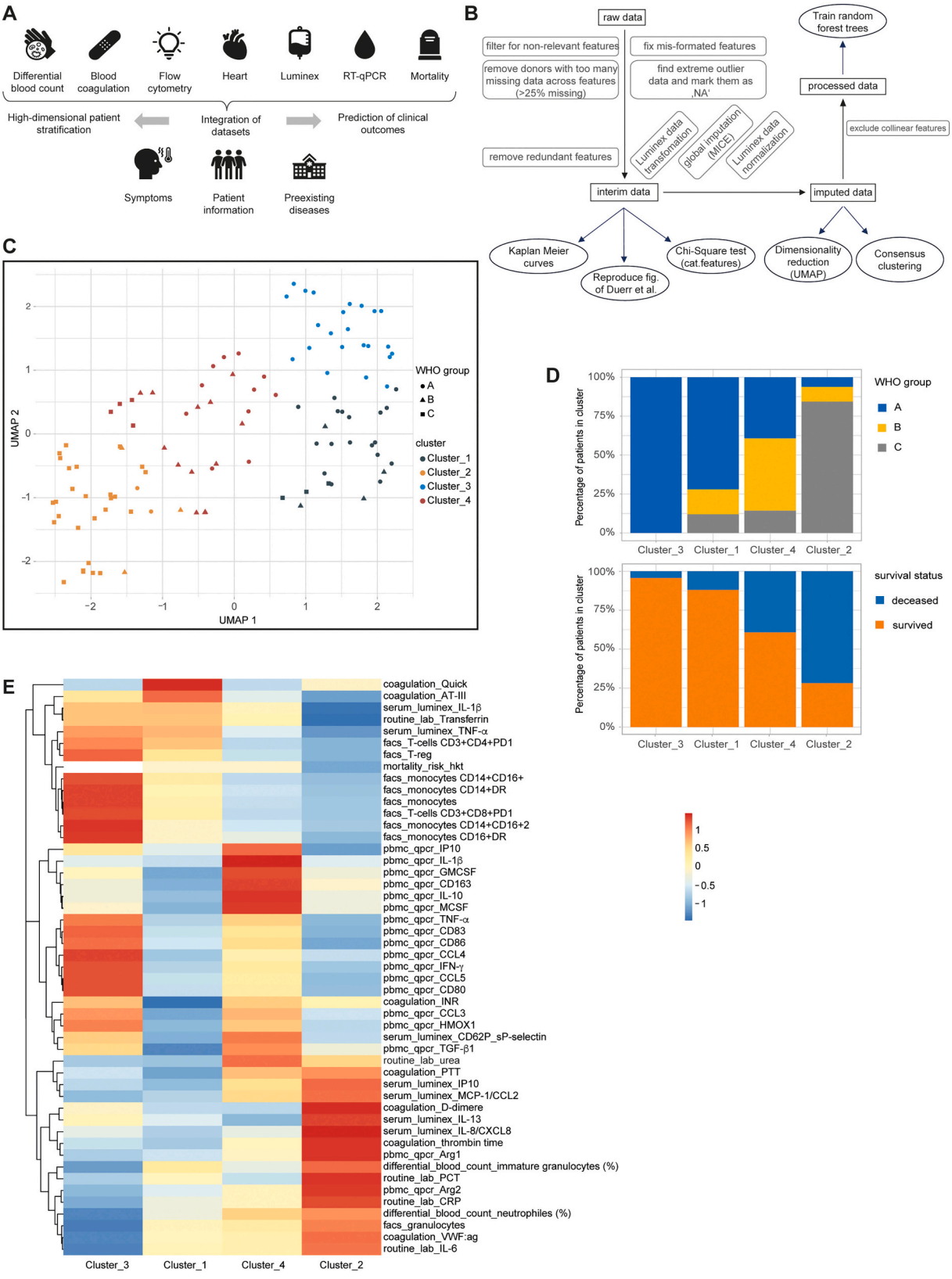

(caption on next page)

Fig. 1. Unbiased assessment of patient stratification using clinical and patient data. (A) Overview of available data types included in the dataset from study cohort. (B) Overview of analysis steps; Following data integration datasets have been used for unbiased stratification and the prediction of clinical outcomes. Strategy is depicted as flow scheme. (C) UMAP representation of patients included in the study. Colors indicate results of consensus clustering of the integrated dataset; shape according to WHO classification; Dimensionality reduction based on the integrated dataset. (D) Bar charts showing the composition of the identified clusters; Distribution of patients after clustering based on the integrated datasets into cluster 1–4. Upper graph shows the proportion of the different WHO categories per cluster; lower graph shows the survival status per cluster. (E) Heatmap representation of features identified as being differential between clusters. Rows of the heatmap are clustered hierarchically. The colors represent a z-transformed mean value of the respective features. (AT III: antithrombin III; PBMC: peripheral blood mononuclear cells; Il1-β: interleukin 1β; TNF-α: tumor necrosis factor α; FACS: fluorescence activated cell sorting; T-reg: regulatory T cells; IP10: interferon-γ induced protein 10 kD/CXCL10; GMCSF: granulocyte/macrophage colony-stimulating factor; IL-10: interleukin 10; RT-qPCR: Quantitative reverse transcription polymerase chain reaction; MCSF: macrophage colony-stimulating factor; CCL4: CC-chemokine ligand 4; IFN-γ: interferon γ; CCL5: CC-chemokine ligand 5; CCL3: CC-chemokine ligand 3; HMOX1: heme oxygenase 1; CD62P_sP-selectin: soluble P-selectin; TGF-β1: transforming growth factor β1; CCL2: CC-chemokine ligand 2; IL-13: interleukin 13; IL-8: interleukin 8; Arg1: arginase type I; PCT: procalcitonin; Arg2: arginase type II; CRP: C reactive protein; VWF:ag: von Willebrand factor antigen; IL-6: interleukin 6).

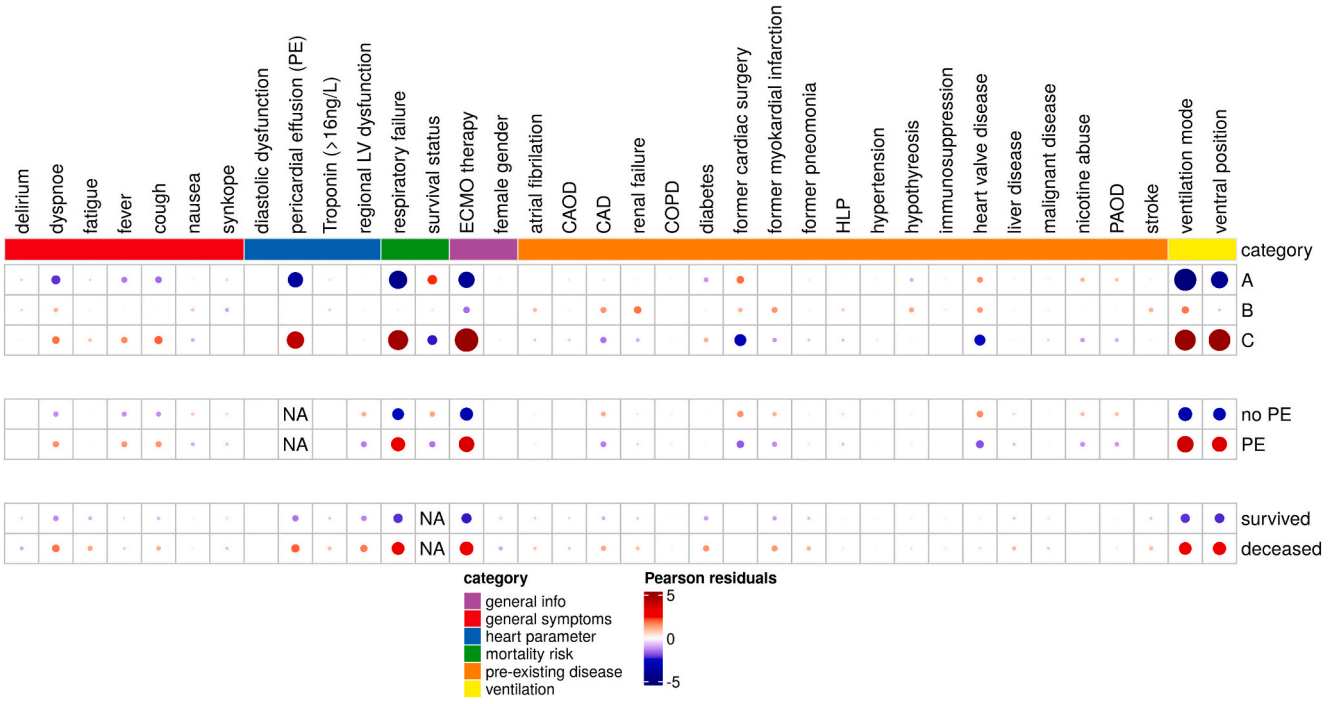

Fig. 2. Dot plot of calculated Pearson residuals to check for possible positive (positive residuals) or negative (negative residuals) associations between two categorical variables. Pearson residuals of categorical variables on WHO associated categories (A, B C), presence or absence of pericardial effusion (PE) and survival status are shown. The size and color of the dots represent the strength of the association between two variables. The larger the dot, the more important is the feature for the respective variables. Positive residuals are in red. Positive values a positive association between the corresponding feature and e.g. the WHO group. Negative residuals are in blue and indicate negative association. (COAD: central obstructive arterial disease; CAD: coronary arterial disease; COPD chronic obstructive pulmonary disease; POAD: peripheral obstructive arterial disease).

separation between PE and no PE patients than monocytes alone. No significant difference in CD3+ CD8+ T cell numbers in both subgroups could be observed (Fig. 3I). Regulatory T cells were reduced in PE patients (Wilcoxon $p = 0.00072$; Fig. 3Γ`).

3.3. AI-composed parameters for more precise prediction of COVID-19 severity

Finally, we used the complete dataset (both continuous and discrete data) to perform prediction analysis. As in multiple independent study populations presence of PE over the course of SARS-CoV-2-infection was associated with a reduction of survival (Fig. 3A), PE-patients were considered as a population at risk due to most likely virus induced myocardial damage. Therefore, parameters associated with presence of PE in COVID-19 patients were assumed to not only serve as prognostic tools but also as group characteristics uncovering underlying etiological mechanisms. To benefit from the abundance of available data, we followed a machine-learning approach based on random forest trees (RFT) extending the previous immunological focus (CD14 + HLA-DR+ monocytes) to clinical features (categorical and continuous).

In Fig. 4B AI-detected 30 most important features were listed according to their relevance for the separation into PE and non-PE patients. C-reactive protein served as the most important parameter, whereas CD14 + HLA-DR+ monocytes were placed tenth. All features listed demonstrated significant differences between PE and non-PE COVID-19 patients exemplarily shown for the top 11 in Fig. 4A.

To assess which prognostic parameter (RFT-selected features, CD14 + HLA-DR+ monocytes, CD8/Treg/monocyte ratio) provides the best classification between PE and non-PE, we compared logistic regression and the random forest model on a test dataset. Logistic regression, chosen for its interpretability and clinical relevance, demonstrated the robustness of the features across different modelling paradigms. While CD14 + HLA-DR+ monocytes alone were strong predictors, RFT-selected features achieved the best AUC (both in logistic regression AUC and RFT AUC) (Fig. 4C). Already indicated by its lower significance (Fig. 3I) CD8/Treg/monocyte ratio performed inferior.

Taken together, Fig. 4 includes ROC curves for both RFT and logistic regression. This shows that selected features perform well in the model

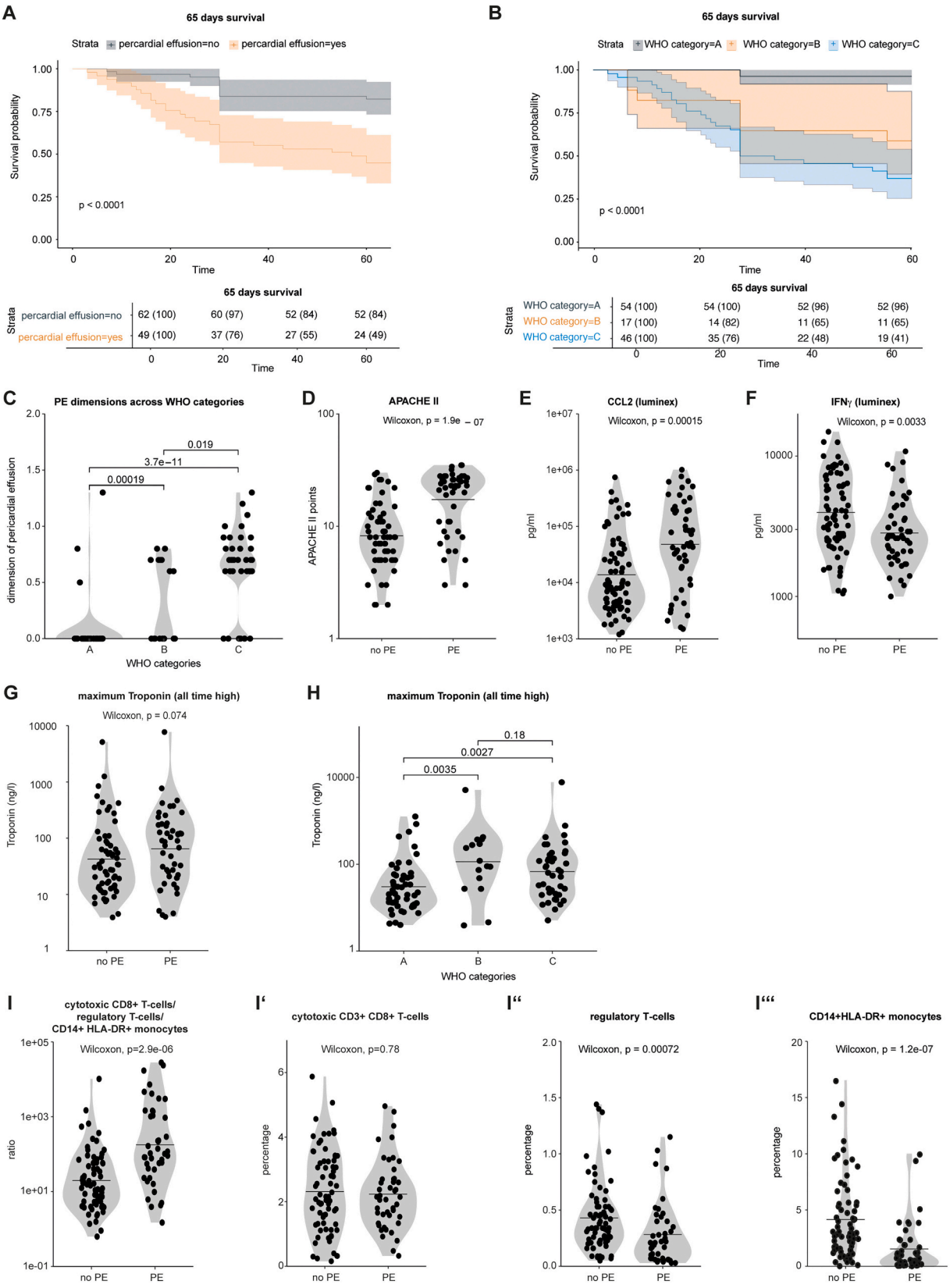

Fig. 3. Continuous data in the dataset are used to test the hypotheses/results from Duerr et al. (2020). (A-B) Kaplan Meier Plots for the variables "pericardial effusion" (PE) and "WHO-associated categories". (C—H) Violin plots showing different parameters present in the dataset. In addition, the corresponding values for each donor are shown as points. Wilcoxon test was used to compare two variables. (I) Violin plot showing the statistics based on the quotient of Duerr et al. [1] (I′, I″, I‴) Violin plots showing the cell count statistics used for quotient calculation in (I). For (I–I‴), the values for each donor are shown as points. Wilcoxon test was used to compare two variables. (APACHE II: clinical rating system to evaluate morbidity and mortality of ICU patients; CCL2: CC-chemokine ligand 2; IFN-γ: Interferon γ).

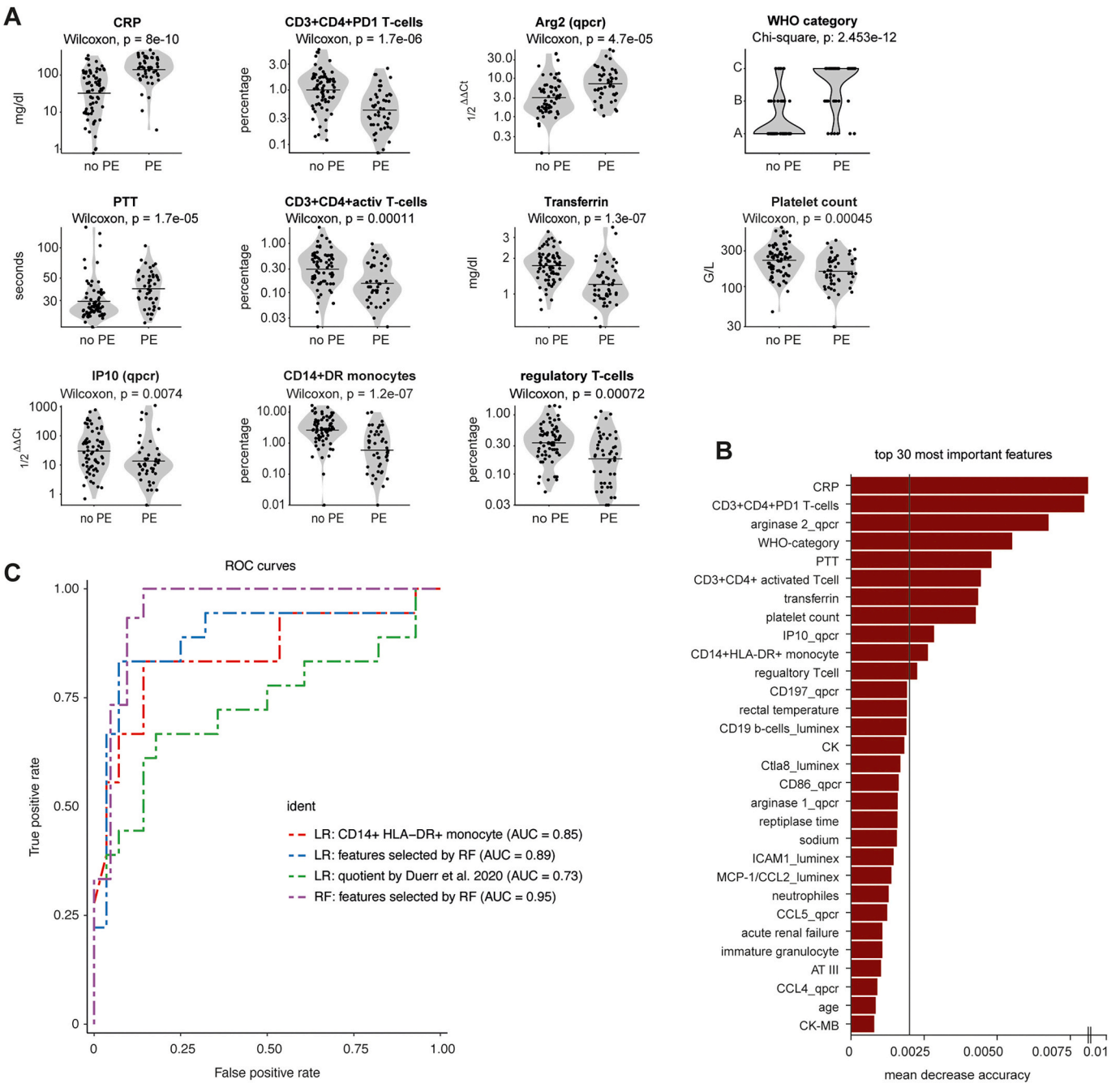

Fig. 4. (A) Violin plots of the identified most important features in the dataset to predict (PE). The corresponding values for each donor are shown as points. For two-variables comparisons, Wilcoxon test was used; for multi-comparisons, Kruskal-Wallis test was used; for categorical comparisons Chi-square test was used. (B) Bar plots showing the feature importance, represented by mean decrease accuracy. The vertical line at 0.002 indicates the cutoff used, above which a feature was defined as important for predicting PE. (C) ROC curves to predict PE based on logistic regression. (CRP: C reactive protein; Arg2: arginase type II; PBMC: peripheral blood mononuclear cells; IP10: interferon-γ induced protein 10 kD/ CXCL10; ROC curve: receiver-operating-characteristics curve; CK: creatine kinase; Ctla8: interleukin-17 A; ICAM1: intercellular adhesion molecule 1/CD54; CCL5: CC-chemokine ligand 5; AT III: antithrombin III; CCL4: CC-chemokine ligand 4; CK-MB: creatine kinase-MB; LR: logistic regression; RF: random forest).

that identified them and remain robust across models. This dual evaluation emphasizes the reliability and generalizability of the selected features.

Since the use of random forest trees appeared promising for the detection of the most important features separating PE and non-PE, we also applied the approach to identify features predicting SWOSS category and survival status (Fig. 5). In line with PE, CRP was the most important parameter for SWOSS group allocation (Fig. 5A,B). While CD14 + HLA-DR+ monocytes were ranked as an important factor, the RFT-algorithm detected presence of PE as a less relevant parameter within the totality of potential prognostic data in the context of SWOSS (Fig. 5B).

Interestingly, machine-learning revealed SWOSS as the most important feature bearing the potential of survival prediction (Fig. 5C, D). While CRP was ranked 6th neither PE nor CD14 + HLA-DR+ monocytes were classified among the top 30 most relevant parameters, as described in Fig. 5B and D.

The individual position of features like PE and CD14 + HLA-DR+

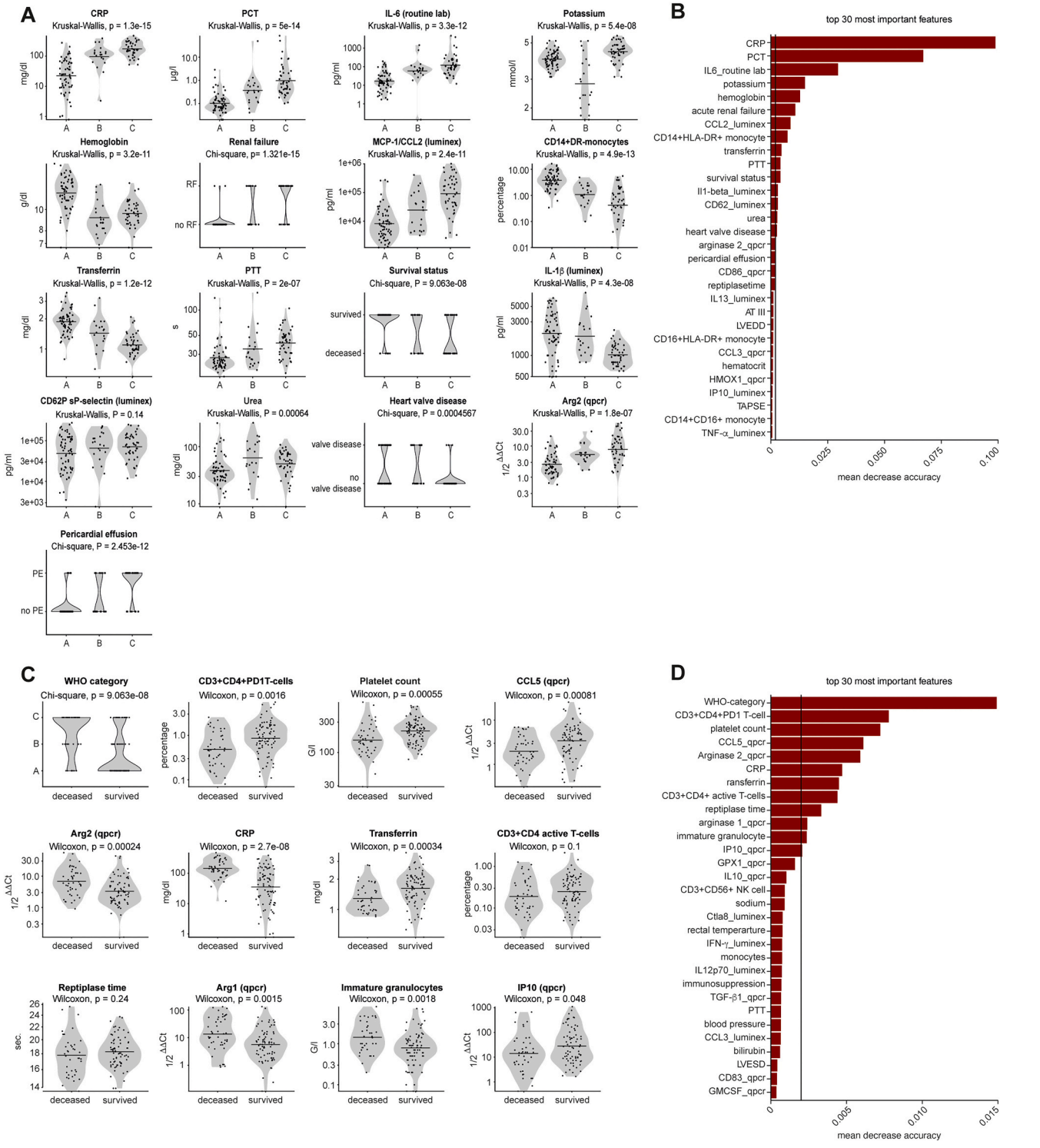

Fig. 5. (A) Violin plots of the identified most important features in the dataset to predict "WHO-associated" categories. The corresponding values for each donor are shown as points. For two-variables comparisons, Wilcoxon test was used; for multi-comparisons, Kruskal-Wallis test was used; for categorical comparisons Chi-square test was used. (B) Bar plots showing the feature importance, represented by mean decrease accuracy. The vertical line at 0.002 indicates the cutoff used, above which a feature was defined as important for predicting "WHO-associated categories. (C) Violin plots of the identified most important features in the dataset to predict survival status. The corresponding values for each donor are shown as points. For two-variables comparisons, Wilcoxon test was used; for multi-comparisons, Kruskal-Wallis test was used; for categorical comparisons Chi-square test was used. (D) Bar plots showing the feature importance, represented by mean decrease accuracy. The vertical line at 0.002 indicates the cutoff used, above which a feature was defined as important for predicting survival status. (CRP: C reactive protein; PCT: procalcitonin; IL6: interleukin 6; CCL2: CC-chemokine ligand 2; Il-1β: interleukin 1β; IL13: interleukin 13; AT III: antithrombin III; LVEDD: left ventricular enddiastolic diameter; CCL3: CC-chemokine ligand 3; HMOX1: heme oxygenase 1; IP10: interferon-γ induced protein 10 kD/CXCL10; TAPSE: tricuspid annular plane systolic excursion; TNF-α: tumor necrosis factor α; CCL5: CC-chemokine ligand 5; GPX1: glutathione peroxidase 1; Ctla8: interleukin-17 A; IFN-γ: interferon γ; IL 12p70: bioactive interleukin 12; TGF-β1: transforming growth factor β1; LVESD: left ventricular end systolic diameter; GMCSF: granulocyte/macrophage colony-stimulating factor).

monocytes within the AI-composed conglomerates for the prediction of PE, SWOSS, and survival must not be interpreted as inconsistent with previously reported, highly significant results (Fig. 3A, I') as taken alone these parameters perform inferior in terms of prediction statistics compared to the multivariate RFT-generated prognostic tools.

4. Discussion

During the COVID-19 pandemic, given its tremendous impact on global health, a rapid increase in understanding and insight of this new disease, its etiology, its clinical course and its treatment options were urgently needed. Driven by time pressure and rising numbers of deaths, scientific findings were often based on rather low case numbers and few diagnostic methods. In our previous publication in 2020, based on 19 patients, we were able to identify PE and (in PE-patients) CD8/Treg/monocyte ratio as potential prognostic parameters predicting a severe course of disease. [1] After abatement of the initial threat situation, in the meanwhile we could rely our results on an increase of case volume to 7-fold (134), perform in depth immunological characterization of all patients and review our recent preliminary findings with the help of machine learning-analyses.

Unbiased clustering of patient characteristics resulted in previously stated and on clinical expertise-based summary of the WHO ordinal severity scale (SWOSS) into groups A [1–4], B (5 + 6) and C (7 + 8). [1]

While previously small retrospective studies of critically ill patients reported high incidences of AP and consequently presence of PE, results of a large retrospective analysis suggest an incidence of PE of 0.46 % within the spectrum of in-hospital COVID-19 patients. [12,17,18]

In line with Li et al., mortality, severity of disease (APACHE II), and inflammation (CCL 2, IFN-γ) were strongly associated with the presence of PE (Fig. 3A), indicating AP. Moreover, concomitant morbidities in AP patients, such as renal failure, were comparable between the study populations. [12] Previously, CD8/Treg/monocyte ratio was considered as a good prognostic factor. [1] In the present study, ROC curve analysis revealed CD14 + HLA-DR+ monocytes alone as a more sensitive and specific predictor for the occurrence of PE and subsequently morbidity and mortality (Fig. 4C). Moreover, inclusion of clinical parameters according to machine learning-algorithms (e.g. CRP, Arg2 [for more features see Fig. 5B]) results in an even better sensitivity-to-specificity tradeoff predicting not only the presence of PE but also SWOSS category and survival. Of note, RFT-features detected as important for each endpoint must be interpreted in the context of a multivariate analysis. Therefore, CD14 + HLA-DR+ monocytes and CD8/Treg/monocyte ratio cannot be compared with single parameters of the AI-selection such as CRP, but rather need to be acknowledged as relevant standalone prognostic parameters (as depicted in Fig. 4C).

Notably, we aimed for an unbiased analysis of the data using machine learning and identified a set of features that are useful for predicting PE in clinical settings. However, some of the parameters we identified, such as survival, are not clinically applicable as predictive tools, as they can only be determined retrospectively. Nevertheless, these findings provide a critical foundation for the development of robust multivariate prediction models. While the AI-detected prognostic features of this study might serve as promising starting points for further mechanistic decryption of the interplay between COVID-19 and heart disease, this study offers a variety of tools for the identification of COVID-19 patients with prognostically relevant acute myocardial damage for everyday clinical practice, especially. In line with Li et al. and our previous findings, PE serves as an easy-to-access parameter identifying SARS-CoV-2 positive patients at risk. [1,12] As PE size is associated with SWOSS category (Fig. 3C), PE might bear the potential to serve as even more than a dichotomous parameter, stratifying risk for cardiac damage within COVID-19 patients. Taken together, standalone features, e.g., CD14 + HLA-DR+ monocytes and CD8/Treg/monocyte ratio represent biomarkers complementary to PE diagnostic, thereby reinforcing the informative value of PE as a sign of myocardial involvement. Despite the already high precision of our suggested items, the detection of true positive high-risk patients can be further improved by utilizing the RFT-based multivariate conglomerates. However, clinicians can refer to this well-equipped toolbox with the potential to adapt diagnostic precision according to the individual clinical setting.

In the context of AI-based big data analysis, the integration of virus species and environmental factors to our data set bears the potential to result in even greater prognostic accuracy for the detection of cardiac manifestations in COVID-19. [19]

4.1. Limitations

As this is a single center study, we are aware of limitations within our study population. Hence, as reported by Gianfrancesco et al. (e.g. cases of missing data, small sample size, potential misinformation), we performed extensive data cleanup to enhance the robustness and reliability of the data used in our analyses. [20]

The scope of this study was the AI-assisted detection of outcome-relevant parameters beyond the restriction of assumed molecular mechanisms in COVID-19 patients. From a mechanistic perspective, the most relevant hypotheses on how SARS-CoV-2 can provoke pericardial effusion have been published previously and include inflammatory, receptor-mediated, and hypoxic pathways.

First, a widely accepted hypothesis proposes that SARS-CoV-2 induces a severe cytokine storm, leading to systemic inflammation that can extend to the heart and pericardium, causing effusion. Elevated pro-inflammatory cytokines such as IL-6, IL-1β, and TNF-α damage cardiac tissues and contribute to pericardial inflammation and fluid accumulation. [21]

Second, the virus's binding to ACE2 receptors, which are present on myocardial and pericardial cells, may contribute to direct cardiac damage. Although viral replication in the heart is limited, the ACE2 interaction triggers an immune response that can cause myocarditis or pericarditis, indirectly leading to effusion. [22]

Third, hypoxia resulting from severe COVID-19 respiratory complications can lead to indirect myocardial injury. Elevated troponin levels and stress-related myocardial injury increase susceptibility to pericardial effusion, especially in severe cases.

Supplementary data to this article can be found online at https://doi.org/10.1016/j.lfs.2025.123524.

CRediT authorship contribution statement

G.D. Duerr: Writing – review & editing, Writing – original draft, Visualization, Validation, Supervision, Project administration, Methodology, Investigation, Funding acquisition, Formal analysis, Data curation, Conceptualization. **M. Hamiko:** Writing – review & editing, Validation, Supervision, Software, Resources, Methodology, Investigation, Formal analysis, Data curation. **J. Beer:** Writing – review & editing, Writing – original draft, Visualization, Validation, Supervision, Software, Project administration, Methodology, Investigation, Formal analysis, Data curation. **J. Nattermann:** Validation, Resources, Methodology. **M. Schafhaus:** Software, Formal analysis. **S.A.E. Held:** Writing – review & editing, Methodology, Formal analysis. **J.C. Schewe:** Writing – review & editing, Validation, Resources, Data curation. **M. Wittmann:** Writing – review & editing, Validation, Resources, Project administration, Investigation. **C. Kurts:** Writing – review & editing, Software, Resources, Investigation, Funding acquisition. **S. Zimmer:** Writing – review & editing, Validation, Resources, Investigation, Data curation. **M. Velten:** Writing – review & editing, Supervision, Resources, Investigation, Funding acquisition, Formal analysis, Data curation, Conceptualization. **A. Heine:** Writing – review & editing, Writing – original draft, Visualization, Validation, Supervision, Project administration, Methodology, Funding acquisition, Formal analysis, Data curation, Conceptualization.

Funding

German Heart Research Foundation, Grant No.: F27/20: to Duerr GD, Velten M, Heine A, Kurts C.

Declaration of competing interest

The authors declare the following financial interests/personal relationships which may be considered as potential competing interests:

Georg Daniel Duerr reports financial support was provided by German Heart Research Foundation. If there are other authors, they declare that they have no known competing financial interests or personal relationships that could have appeared to influence the work reported in this paper.

Acknowledgments

We thank Christine Peigney, Chrystel Flores, and Sandra Hüwe for their expert assistance in conducting the molecular and FACS experiments. Our special thanks go to Kevin Baßler and Patrick Günther from aimed analytics GmbH for the extremely meticulous data processing and statistical analysis.

The work received funding from the German Heart Research Foundation, Grant No.: F27/20: to Duerr GD, Velten M, Heine A, Kurts C.

References

[1] G.D. Duerr, A. Heine, M. Hamiko, S. Zimmer, J.A. Luetkens, J. Nattermann, et al., Parameters predicting COVID-19-induced myocardial injury and mortality, Life Sci. 260 (2020) 118400.
[2] M.G. Friedrich, L.T. Cooper Jr., What we (don't) know about myocardial injury after COVID-19, Eur. Heart J. 42 (19) (2021) 1879–1882.
[3] S.X. Gu, T. Tyagi, K. Jain, V.W. Gu, S.H. Lee, J.M. Hwa, et al., Thrombocytopathy and endotheliopathy: crucial contributors to COVID-19 thromboinflammation, Nat. Rev. Cardiol. 18 (3) (2021) 194–209.
[4] A. Aleksova, A.L. Fluca, G. Gagno, A. Pierri, L. Padoan, A. Derin, et al., Long-term effect of SARS-CoV-2 infection on cardiovascular outcomes and all-cause mortality, Life Sci. 310 (2022) 121018.
[5] B. Siripanthong, B. Asatryan, T.C. Hanff, S.R. Chatha, M.Y. Khanji, F. Ricci, et al., The pathogenesis and long-term consequences of COVID-19 cardiac injury. JACC: basic to translational, Science 7(3, Part 1):294-308 (2022).
[6] P. VasanthiDharmalingam, V. Karuppagounder, K. Watanabe, H. Karmouty-Quintana, S.S. Palaniyandi, A. Guha, et al., SARS–CoV-2 mediated Hyperferritinemia and cardiac arrest: preliminary insights, Drug Discov. Today 26 (5) (2021) 1265–1274.
[7] Negron SG, Kessinger CW, Xu B, Pu WT, Lin Z. Selectively expressing SARS-CoV-2 Spike protein S1 subunit in cardiomyocytes induces cardiac hypertrophy in mice. bioRxiv. 2021:2021.06.20.448993.
[8] T. Aikawa, H. Takagi, K. Ishikawa, T. Kuno, Myocardial injury characterized by elevated cardiac troponin and in-hospital mortality of COVID-19: an insight from a meta-analysis, J. Med. Virol. 93 (1) (2021) 51–55.
[9] D. Mathew, J.R. Giles, A.E. Baxter, D.A. Oldridge, A.R. Greenplate, J.E. Wu, et al., Deep immune profiling of COVID-19 patients reveals distinct immunotypes with therapeutic implications, Science 369 (6508) (2020).
[10] D. Lindner, A. Fitzek, H. Bräuninger, G. Aleshcheva, C. Edler, K. Meissner, et al., Association of Cardiac Infection with SARS-CoV-2 in confirmed COVID-19 autopsy cases, JAMA Cardiol. 5 (11) (2020) 1281–1285.
[11] M. Ali, H.A. Shiwani, M.Y. Elfaki, M. Hamid, R. Pharithi, R. Kamgang, et al., COVID-19 and myocarditis: a review of literature, The Egyptian Heart Journal. 74 (1) (2022) 23.
[12] P. Li, A. Shi, X. Lu, C. Li, P. Cai, C. Teng, et al., Incidence and impact of acute pericarditis in hospitalized patients with COVID-19, J. Am. Heart Assoc. 12 (20) (2023) e028970.
[13] N.R. Blagojevic, D. Bosnjakovic, V. Vukomanovic, S. Arsenovic, J.S. Lazic, M. Tadic, Acute pericarditis and severe acute respiratory syndrome coronavirus 2: case report, Int. J. Infect. Dis. 101 (2020) 180–182.
[14] B. Bhandari, S. Neupane, R. Khanal, K. Lnu, Y. Wert, S. Komanduri, COVID-19 pericarditis mimicking an acute myocardial infarction: a case report and review of literature, J. Community Hosp. Intern. Med. Perspect. 11 (3) (2021) 315–321.
[15] G.H. Alay, D. Tatlisuluoglu, K. Bulut, B.I. Fikri, A. Oztas, G. Turan, The relationship between immature granulocyte count and mortality in ARDS due to COVID-19, Niger. J. Clin. Pract. 25 (8) (2022) 1301–1307.
[16] V.E. Georgakopoulou, S. Makrodimitri, M. Triantafyllou, S. Samara, P. M. Voutsinas, A. Anastasopoulou, et al., Immature granulocytes: innovative biomarker for SARS-CoV-2 infection, Mol. Med. Rep. 26 (1) (2022).
[17] D. Doyen, P. Dupland, L. Morand, E. Fourrier, C. Saccheri, M. Buscot, et al., Characteristics of cardiac injury in critically ill patients with coronavirus disease 2019, CHEST 159 (5) (2021) 1974–1985.
[18] Y. Liu, J. Xie, P. Gao, R. Tian, H. Qian, F. Guo, et al., Swollen heart in COVID-19 patients who progress to critical illness: a perspective from echo-cardiologists, ESC Heart Failure. 7 (6) (2020) 3621–3632.
[19] C.Y. Tang, C. Gao, K. Prasai, T. Li, S. Dash, J.A. McElroy, et al., Prediction models for COVID-19 disease outcomes, Emerging Microbes & Infections. 13 (1) (2024) 2361791.
[20] M.A. Gianfrancesco, S. Tamang, J. Yazdany, G. Schmajuk, Potential biases in machine learning algorithms using electronic health record data, JAMA Intern. Med. 178 (11) (2018) 1544–1547.
[21] Y. Tang, J. Liu, D. Zhang, Z. Xu, J. Ji, C. Wen, Cytokine storm in COVID-19: the current evidence and treatment strategies, Front. Immunol. 11 (2020).
[22] Avila M. Del Nogal, R. Das, J. Kharlyngdoh, E. Molina-Jijon, H. Donoro Blazquez, S. Gambut, et al., Cytokine storm-based mechanisms for extrapulmonary manifestations of SARS-CoV-2 infection. JCI, Insight 8 (10) (2023).

Referenced from supplementary table 1

[23] H.M.A. Wickham, et al., Welcome to the Tidyverse, J Open Sour Softw. 4 (10.21105) (2019).
[24] Z. Gu, R. Eils, M. Schlesner, Complex heatmaps reveal patterns and correlations in multidimensional genomic data, Bioinformatics 32 (18) (2016) 2847–2849.
[25] A. Liaw, Classification and Regression by randomForest, R news, 2002.
[26] T.M. Therneau, P.M. Grambsch, T.M. Therneau, P.M. Grambsch, The Cox Model, Springer, 2000.
[27] Alboukadel K, Marcin K, Przemyslaw B, Scheipl F. survminer: Drawing Survival Curves using'ggplot2'. R package version 04. 2019;4.
[28] J. Friedman, T. Hastie, R. Tibshirani, Regularization paths for generalized linear models via coordinate descent, J. Stat. Softw. 33 (1) (2010) 1.
[29] Kuhn M, Wing J, Weston S, Williams A, Keefer C, Engelhardt A, et al. caret: classification and regression training. 2020. R package version. 2021;3.
[30] Kolde R. Pheatmap: pretty Heatmaps. R package version 1.0. 12. 2019.
[31] S. Van Buuren, K. Groothuis-Oudshoorn, Mice: multivariate imputation by chained equations in R, J. Stat. Softw. 45 (2011) 1–67.
[32] T. Sing, O. Sander, N. Beerenwinkel, T. Lengauer, ROCR: visualizing classifier performance in R, Bioinformatics 21 (20) (2005) 3940–3941.
[33] P. Du, W.A. Kibbe, S.M. Lin, lumi: a pipeline for processing Illumina microarray, Bioinformatics 24 (13) (2008) 1547–1548.
[34] Melville J, Lun A, Djekidel MN, Hao Y. uwot: The uniform manifold approximation and projection (UMAP) method for dimensionality reduction. R package version 01. 2020;10.
[35] T.L. Pedersen, Patchwork: The Composer of Plots, Contributed Packages, CRAN, 2019.
[36] S. Lê, J. Josse, F. Husson, FactoMineR: an R package for multivariate analysis, J. Stat. Softw. 25 (2008) 1–18.
[37] D.S. Chiu, A. Talhouk, diceR: an R package for class discovery using an ensemble driven approach, BMC bioinformatics. 19 (2018) 1–4.
[38] David Sjoberg, ggsankey: Sankey, Alluvial and Sankey Bump Plots 564 (2022).